Proceedings of the ASME 2018 13th International Manufacturing Science and Engineering Conference
MSEC2018
June 18-22, 2018, College Station, TX, USA

MSEC2018-6572

AUTOMATED FIBER EXTRACTION FROM SEM IMAGES WITH APPLICATION TO QUALITY CONTROL OF FIBER-REINFORCED COMPOSITES MANUFACTURING

Md. Fashiar Rahman[1], Jianguo Wu[2*], Bill Tseng[3]
[1]Computational Science Program, UTEP, Texas 79968, USA
[2*]Corresponding author, Department of Industrial Engineering and Management, Peking University, Beijing, China, 100871, Email: j.wu@pku.edu.cn
[3]Industrial, Manufacturing and Systems Engineering, UTEP, Texas 79968, USA

KEYWORDS

Fiber reinforced composites; image segmentation; Hough Transform; image morphology; quality control

ABSTRACT

The morphology of fibers (e.g., spatial uniformity and orientation) plays a decisive role in determining the material properties or fabrication quality of fiber-reinforced nanocomposites. The existing literature lacks a reliable and automatic fiber extraction method for morphology analysis based on the scanning electron microscope (SEM) images. This paper proposes four different methods, namely, the simple Hough Transform, opening method, partitioning Hough Transform and gradient based Hough Transform, to automatically identify the fibers from SEM images to expedite the morphology analysis. The performance of these methods are thoroughly evaluated and compared through simulation studies and real case studies.

INTRODUCTION

Fiber-reinforced composites are hybrid materials where micro- or nano-scaled axial particulates are embedded into a matrix material. They are being increasingly used as alternatives to the conventional materials in various application domains because of their superior mechanical properties [1, 2], e.g., high strength, high stiffness and light weight, and many other functional properties, such as high energy density in capacitors [3]. The spatial homogeneity and oriental alignment of fibers in the base material play a decisive role in determining the final properties of composites. For composites with well-aligned fibers, the longitudinal tensile strength along the fiber aligning orientation will be much higher than the transverse strength [4]. Whereas with randomly aligned fibers, the composites will be isotropic and may be cheaper to fabricate than those with aligned fibers. In some applications, random orientation may be desirable to achieve the best isotropic mechanical properties. However, in some other applications, well-aligned fibers may be more preferable. Recently research showed that well-aligned fillers can significantly enhance the dielectric properties of the base material, specifically the dielectric permittivity and breakdown strength [5-7]. Besides the alignment, the spatial distribution is also crucial for material properties. Almost in all applications, the homogeneous spatial distribution of fibers in the specimen is desired. Similar to particle-reinforced nanocomposites [8-11], the clustering or aggregation of fibers often exist due to imperfectly controlled processing, which may significantly influence the properties and reduce the performance [12].

Nowadays, the standard quality inspection technique is morphology analysis of fibers imbedded in the base material based on SEM images. This analysis is often based on visual inspection of microscopic images, which is often time consuming and subjective. Besides, to get a reliable quantitative quality evaluation, the fiber location, size, and orientation are often needed. However, it is unrealistic to collect all these information manually. Therefore, automatic fiber extraction from SEM images is highly desirable for quality assessment.

Image processing approaches have been successfully used for the morphology analysis of nanoparticles (circular or elliptical shape) [13-16]. However, there are very limited automated fiber (axial particulates) segmentation and analysis methodologies in the existing literature. Kimura et al. [17] proposed an algorithm to measure the root length through image processing. Kawabata et al. [18] developed an image processing technique to detect and count asbestos fibers. Peng et al. [19] developed algorithms to estimate the length, position and orientation of nanowires in the fluidic workspace from optical section microscopy images. However, all of the three methods

are not applicable to fiber extraction from SEM of composite materials, where fibers are often overlapped or connected with each other. Jeon et al. [20] developed a method to characterizing the nanowire alignment in microchannel using ridge detection, texton analysis and autocorrelation function (ACF) calculation. The texton of different orientation angle is convoluted with the autocorrelation field to detect the distribution of wire alignment. This method can approximately estimate the orientation distribution. However, it is not capable of identifying the fiber locations, which are essential for spatial homogeneity assessment.

In this paper, we developed four different methods, namely, the simple Hough Transform, opening method, partitioning Hough Transform and gradient based Hough Transform, to automatically identify the fibers from SEM images. Hough transform (HT) algorithm has been recognized as a very efficient tool to identify a certain class of shapes, such as lines, circles, and ellipses, by a voting procedure [21]. The classic HT was used to detect straight lines in the image. In this paper, we only consider the straight fibers. Intuitively, the straight fibers can be detected by detecting the long boundaries or by detecting the skeleton after thinning process through simple HT method. However, there are various issues that make the simple HT not effective. This paper proposes several approaches to solve these issues when using the simple HT method. Besides, an opening method is also developed.

The rest of the paper is organized as follows. In Section 2, the four proposed methods are introduced. The simulation study, analysis and results are provided in Section 3. In Section 4, the proposed methods are applied to real SEM images. The conclusion and discussion are provided in Section 5.

METHODOLOGY

In this section, the technical details of the proposed four methods will be introduced.

Opening Method Based Fiber Detection: In this subsection, a method for detecting fiber has been proposed based on the "Opening" [22] operator. The opening of image A by a structuring element (SE) B is denoted (AoB) and is defined as

$$AoB = (A \ominus B) \oplus B \quad (1)$$

Where, $\ominus$ and $\oplus$ denote the "erosion" and "dilation" operation, respectively. Dilation is the morphologic transformation which combines two sets using vector addition of set elements. If A and B are the subset of N-space, the dilation of A by B is denoted by $A \oplus B$ and is defined as

$$A \oplus B = \{c \in E \mid c = a + b \text{ for some } a \in A \text{ and } b \in B\} \quad (2)$$

Conversely, erosion is the morphological transformation which combines two sets using the vector subtraction of set elements. The erosion of A by B is defined by

$$A \ominus B = \{x \in E \mid x + b \in E \text{ for every } b \in B\} \quad (3)$$

In opening method, the structuring element B acts as a probe which moves across the image A and removes the objects that are smaller than SE using erosion operation. Later dilation operation is employed to restores the shape of the reaming objects. However, restoring accuracy highly depends on the type of structuring element and the shape of restoring objects. In this proposed method, we took the line structuring element with certain length. The SE is varied with all possible angles ranging from -89 to 90 and moved over the SEM image to open the nanofibers. Consequently, the nanofibers which are less than the SE are opened. Since the nanofibers are rectangular in shape and are often larger than the SE, a single fiber may be detected multiple times by different SE's with close orientations. As illustrated in Figure 1(a), each fiber has been detected multiple times (marked by boundaries of different colors). Hence we need to merge these fibers or remove the duplicated segmentation. It is obvious that, if a fiber is opened multiple times, their centroids and the orientations will be very close. Based on this fact, we can check the closeness of the opened fibers and keep the desired one. The procedure is depicted in Figure 1 and the algorithm is illustrated in Table 1.

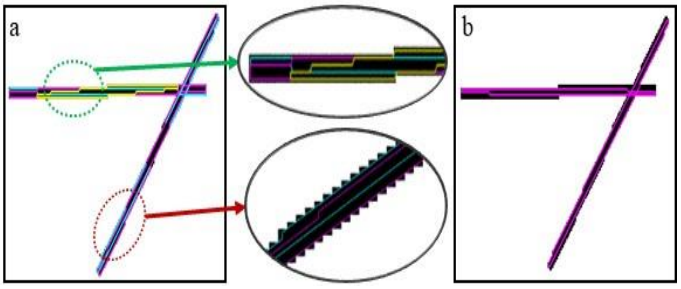

Figure 1. Opening method based fiber detection procedure, (a) detected boundaries after opening operation with duplicated detection (b) duplication deletion

Table 1. Opening based nanofiber extraction

- Convert the SEM image into binary image
- For different angle θ ranging from -89 to 90
  - Perform "Opening" operation on binary image with line structure element with angle θ
  - Find out the boundary of each opened image
  - Extract the centroid and orientation of each opened image
- End
- For all of the orientation
  - Check the closeness of each pair of detected fibers based on their centroid and orientations
  - If closeness of the fibers is below a certain threshold
    - Treat them as a single fiber.
- end

Simple Hough Transform Based Fiber Detection: Hough Transform is a mapping of a line from the spatial domain to another parameter space. It was first introduced by Paul Hough in 1962 [23]. Later it was extended to identify the arbitrary shapes, e.g., circles and ellipse, and it was named "Generalized

Hough Transform" [24]. In Hough Transform, a straight line is represented by the equation

$$\rho = xcos\theta + ysin\theta \quad (4)$$

Where, ρ is the length of the normal vector from the origin to the straight line and θ is the angle it makes with the x axis. The ρ-θ parameter space is subdivided into small accumulator cells to form a two-dimensional matrix. The parameter θ and ρ are usually limited to $\pm\pi / 2$ and $\sqrt{M^2 + N^2}$ respectively, where (M, N) is the image size. Based on this parameterization each image point (x, y) generates a sinusoidal curves in (θ, ρ) space. The points, belongs to a particular line, map to the (θ, ρ) space and intersect at a unique accumulator cell. This accumulator cell identifies the value of ρ and θ for the corresponding line. Thus lines are determined by the intersection of many of these sinusoids. As illustrated in Figure 2, three points $\{(49,1), (25,25), (1,49)\}$ generates three sinusoidal curves *a*, *b* and *c* respectively. Since, these three points belong to the same line, they intersect at a common point d, which gives the parameter of $\rho = 33.9$ and $\theta = 45$ for the corresponding line.

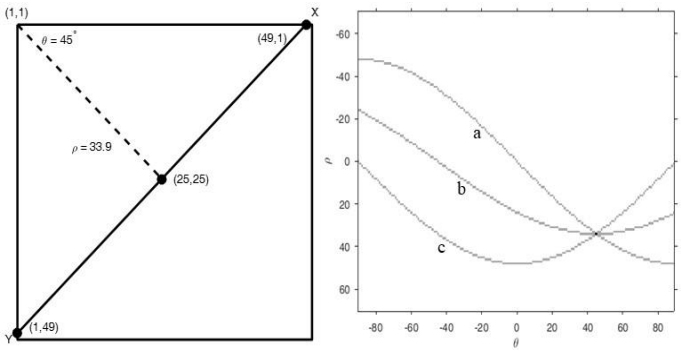

Figure 2. Illustration of Hough Transform

To extract the nanofibers, we could use Hough Transform to detect lines in SEM image. But the direct use of HT generates two major issues. The first issue is that if the fiber is large in width, multiple lines will be detected on the same fiber. Secondly, the accumulator cell can gather points which are in the same line but they are actually from different fibers. To address the first issue, "Skeleton" operation [25] could be used to get the skeletonized image. Given a set point set A, the skeleton operation $S(A)$ is defined as follows:

$$S(A) = \bigcup_{k=0}^{M} S_k(A) \quad (5)$$

$$S_k(A) = (A \ominus kB) - [(A \ominus kB) \ o \ B] \quad (6)$$

Where, M indicates the last iterative step before A erodes to an empty set which defined by equation 4 and k indicates how many times A is eroded ($\ominus$) with the structuring element B and (o) indicates the opening operation.

$$M = \max\{k | (A \ominus kB) \neq \emptyset\} \quad (7)$$

To overcome the second issue, the continuity of the points is evaluated by computing the distance of a pair of point. Then the gap is checked based on a threshold value. If the gap between two sets of point is bigger than the threshold, HT considers them as from separate lines; otherwise they are from the same line.

Partitioning Hough Transform: In Simple HT, "skeleton" operation is employed to alleviate the detection of multiple lines on a single fibers. However, there is still an issue in the above method. The skeleton of other fibers could contribute to the accumulator cell values and may significantly influence the detection accuracy, especially when the density of fiber is very large. To overcome this problem, we propose the partitioning Hough Transform, where the partitioning is first applied to segment SEM images into multiple images based on connected components and then apply Hough transform to each segmented image. The partitioning Hough Transform is illustrated in Table 2.

Table 2. Partitioning Hough Transform for nanofiber segmentation

- Convert the SEM image into binary image
- Partition the binary image into n SEM images with each having one connected component.
- For $i = 1{:}n$
  - Extract the morphological "skeleton" of image i
  - Perform Hough Transform on image i to get the Hough matrix
  - Identify the peaks of the Hough matrix
  - Detect Hough line based on peaks and Hough matrix
- End

Gradient Based Hough Transform: As the density of fibers increases, there would be more fibers crossed with each other. The fiber crossing will significantly influence the shape of the skeleton (from straight lines to curved lines) as shown in Figure 3. Therefore it would reduce the detection accuracy of the HT method.

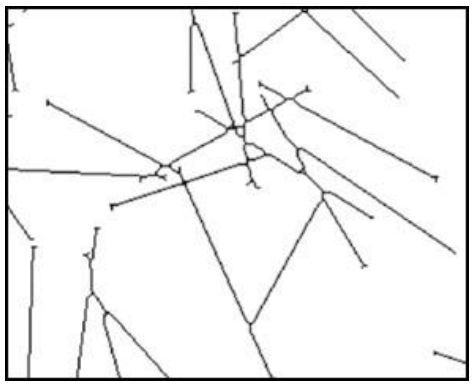

Figure 3. Skeleton of multiple crossed fibers

To solve this issue, another innovative and more effective method is proposed here. This method is the extension of the standard Hough Transform-where each pixel of the fiber boundaries is mapped to a single cell in the discretized (θ, ρ)

space based on its gradient. The rational is that the gradient direction of the fiber boundary is approximately equal to the line orientation θ in Equation 4. Instead of mapping each pixel to a curve in (θ, ρ) space, we only increase the corresponding accumulator with θ equal to the gradient. Using this idea, we can reduce the number of useless votes.

Finding gradient orientation involves two major steps. The first step is to detect the boundary of all fibers and then to measure the changes in x and y coordinates along each boundary. After extracting the gradient information- we can use the gradient based Hough Transform algorithm to detect the boundaries.

Boundaries can be easily extracted through various existing methods, such as "Freeman Chain Code" [26, 27], "Minimum-Perimeter Polygon (MPP)" [28, 29] and "Moore Boundary Tracing Algorithm" [30]. Let g_{x_i} and g_{y_i} be components of the gradient at (x_i, y_i). As the boundary data set (B) is a collection of sequential pairs of x and y coordinates along the boundary, we can easily measure the g_{x_i} and g_{y_i} by taking the difference between two points using equation 8.

$$B = \{(x_i, y_i)\}$$
$$(g_{x_i}, g_{y_i}) = (x_{i+l} - x_i, y_{i+l} - y_i) \quad (8)$$

Where, l is the step size. Then the gradient direction θ for pixel (x_i, y_i) can be calculated by equation 9.

$$\theta_i = \tan^{-1} \frac{g_{y_i}}{g_{x_i}} \quad (9)$$

After finding the gradient orientation, we use these information to detect the fibers using the gradient based Hough Transform. The algorithm is illustrated in Table 3.

Table 3. Gradient based Hough for fiber extraction

- Convert the SEM image into binary image
- Extract the boundaries of fibers
- For each of the boundary pixel (x_i, y_i)
  - Calculate the gradient θ_i
  - Calculate the parameter $\rho_i = x_i cos\theta_i + y_i sin\theta_i$
  - Increase the accumulator $A(\theta_i, \rho_i) = A(\theta_i, \rho_i) + 1$
- End
- Detect the peaks form the Hough matrix *A*
- Find the ρ and θ for the corresponding peaks
- Detect the fibers using corresponding ρ and θ

SIMULATION STUDY

In the following sections, simulated SEM images of fiber reinforced composites are used to evaluate the proposed methods. The image resolution is 2400×1800 pixels. The fibers are uniformly distributed with density $\rho = 0.0001$ fiber/pixel^2. The length of each fiber follows a normal distribution with mean of 120 pixels and standard deviation of 20 pixels. The width is fixed as $2\sigma = 4$ pixels. The intensity of the gray image at each pixel follows a truncated normal distribution within 0 to 255 with 192 ± 32 (mean ± deviation). The fiber orientation is uniformly distributed. Figure 4 shows four simulated SEM images with 50, 100, 200, 400 fibers.

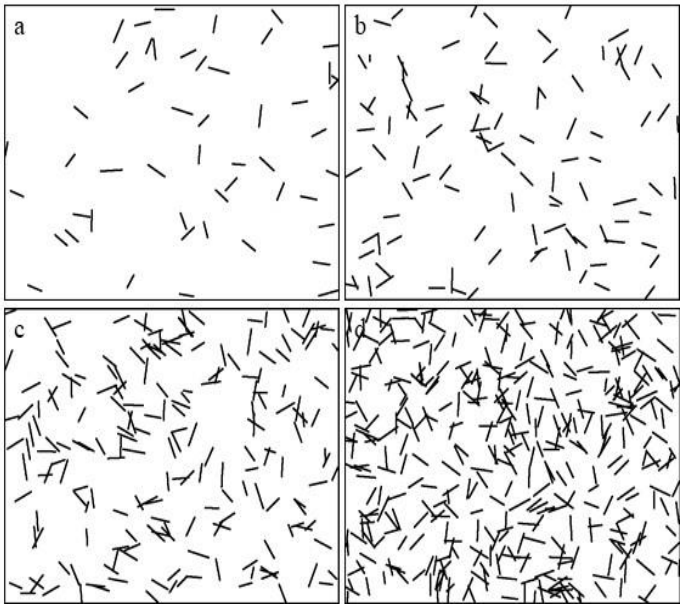

Figure 4. Simulated images (a) 50 fibers (b) 100 fibers (c) 200 fibers (d) 400 fibers

The simple HT method, opening method, partitioning HT method and the gradient based HT method are applied to the simulated image. Figure 5 shows the fiber extraction results by the simple HT method. The result for the opening method, partitioning HT and gradient based HT methods are shown in Figure 6, 7 and 8 respectively. Here the green line indicates the detected fiber while the yellow and red cross specifies the starting and the ending point of the detected line respectively.

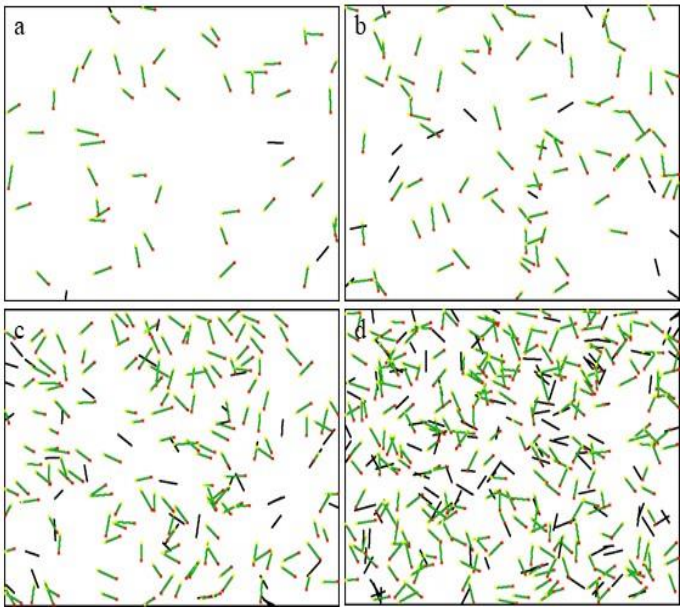

Figure 5. Simple HT method (a) 50 fibers (b) 100 fibers (c) 200 fibers (d) 400 fibers

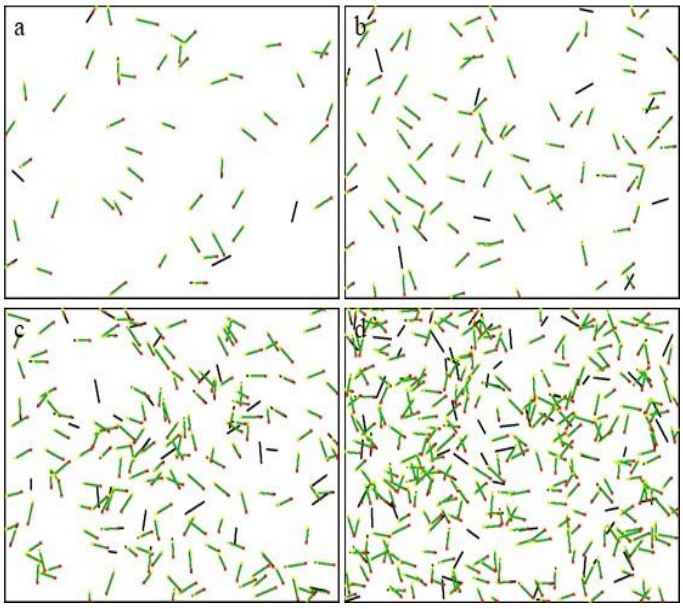

Figure 6. Opening method base HT (a) 50 fibers (b) 100 fibers (c) 200 fibers (d) 400 fibers

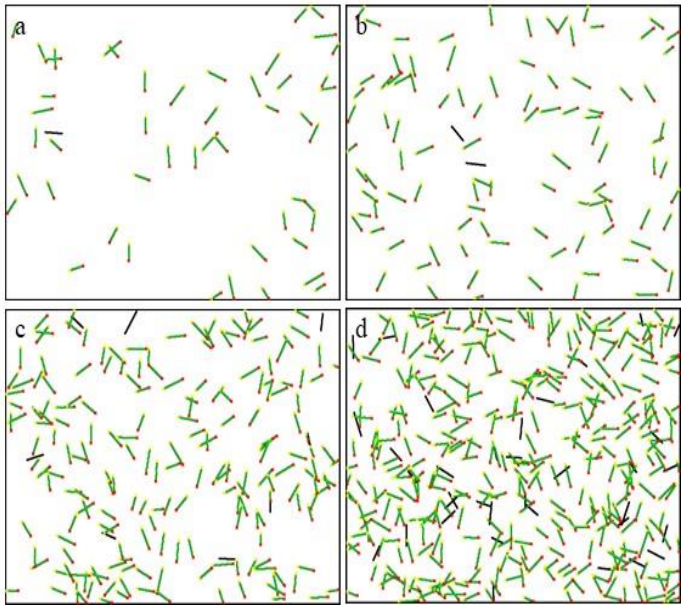

Figure 7. Partitioning HT (a) 50 fibers (b) 100 fibers (c) 200 fibers (d) 400 fibers

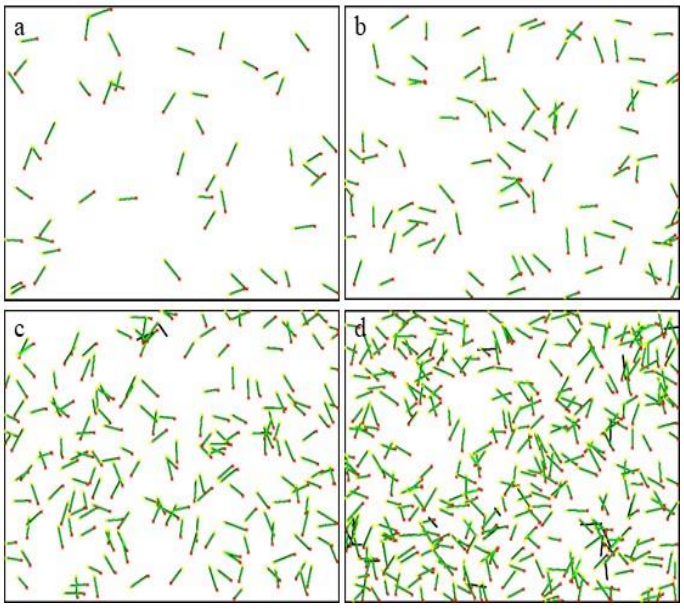

Figure 8. Gradient based HT (a) 50 fibers (b) 100 fibers (c) 200 fibers (d) 400 fibers

The simulation is replicated 30 times. The total number of fibers detected are averaged across the 30 replications for each method. Table 4 and Figure 9 shows the comparison.

Table 4. Extraction results of the four methods

Method	No. of Fibers	Detected Fibers	Accuracy	Maximum error
Simple HT	50	46	0.92	8
	100	88	0.88	16
	200	164	0.82	45
	400	302	0.76	112
Opening Method	50	46	0.92	8
	100	90	0.90	15
	200	180	0.90	28
	400	353	0.88	61
Partitioning HT	50	49	0.98	3
	100	97	0.97	5
	200	188	0.94	19
	400	324	0.81	88
Gradient Based HT	50	50	1	0
	100	100	1	1
	200	198	0.98	4
	400	384	0.96	24

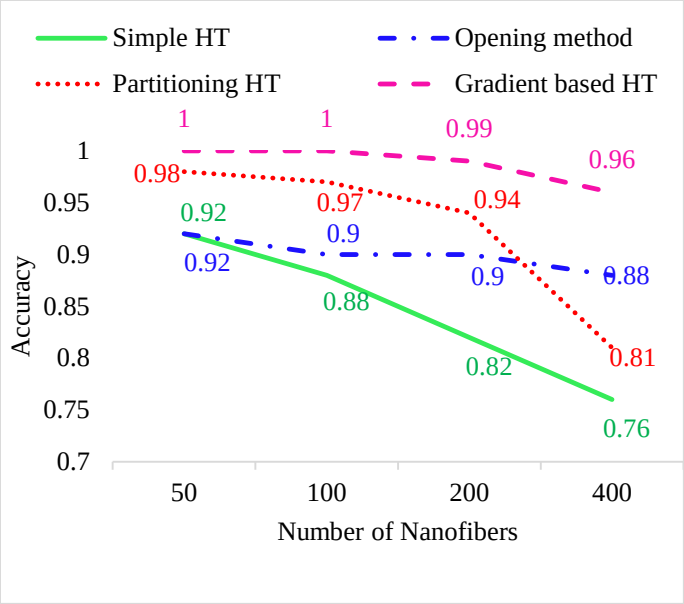

Figure 9. Comparison of the four methods

Clearly, the simple HT method has the lowest extraction accuracy. It is not surprising since some pixels of other fibers on the extension of a fiber will also contribute to the cell of the accumulator that represents this fiber, which will influence the voting accuracy. In comparison, adding the partitioning step before the application of the simple HT could significantly improve the extraction accuracy. However, as the fiber density increases, the extraction accuracy for both methods decreases rapidly. The reason is that, as the fiber density increases, the useless voting by pixels of other fibers increases, which reduces the HT based methods. If the density is too high, most of the fibers may be connected and the partitioning step is no longer working. The extreme case is that all fibers are connected. In such case the partitioning based HT would degenerate to the simple HT method. As expected, the gradient based HT method has the highest accuracy for all the four scenarios, since it could effectively eliminate the useless voting of other fibers when detecting a certain fiber. The opening method is much more stable than the other three methods in terms of the extraction accuracy. When the fiber density is lower, the accuracy of the opening method is not high. However, its advantage becomes obvious as the fiber density goes higher. Therefore, when the fiber density is extreme high, the opening method would be more preferable to all other HT based methods.

APPLICATION TO REAL IMAGES

In this section we apply the proposed methods to extract fibers from two real images, as shown in Figure 10. Here the left image contains 64 fibers and the right image contains 89 fibers.

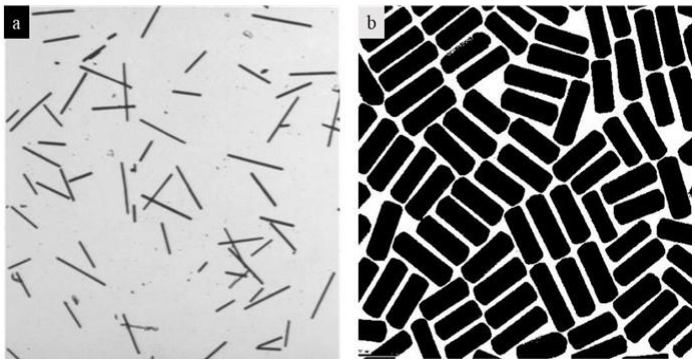

Figure 10. Two real images (a) 64 fibers (b) 89 fibers

Figure 11 shows the extraction results. The first, second, third and fourth row represent the simple HT, opening method, partitioning HT and gradient based HT respectively.

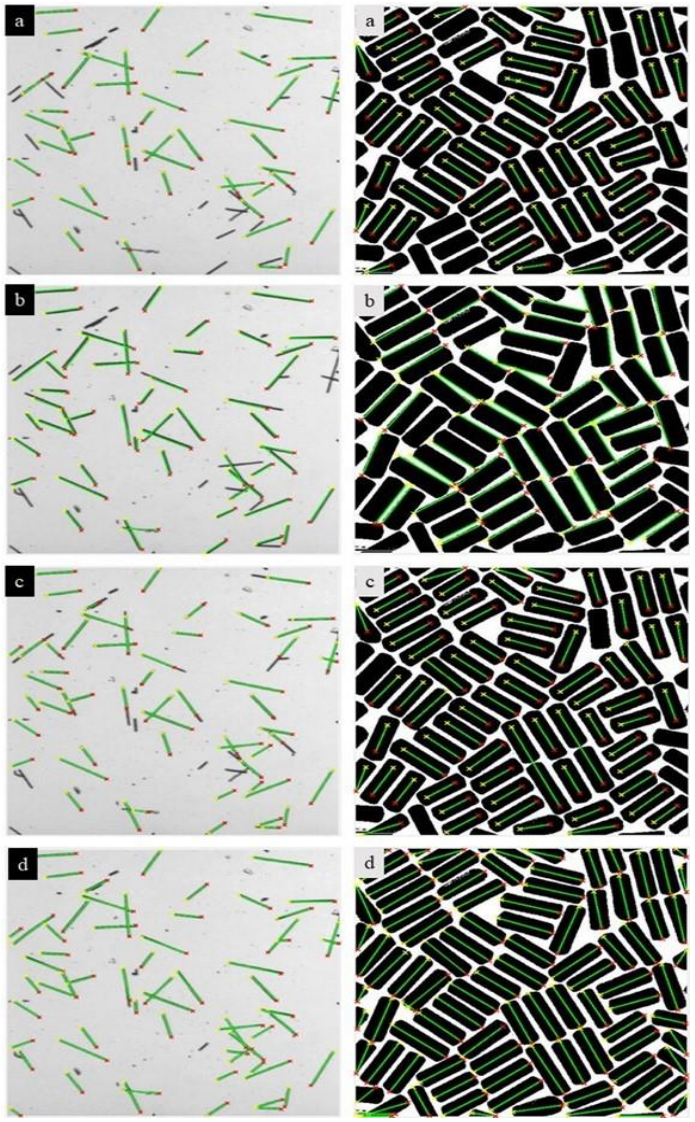

Figure 11 Fiber extraction of real images a) Simple HT b) Opening Method c) Partitioning HT d) Gradient HT

Figure 12 shows the number of detected fibers in two images for each of the methods.

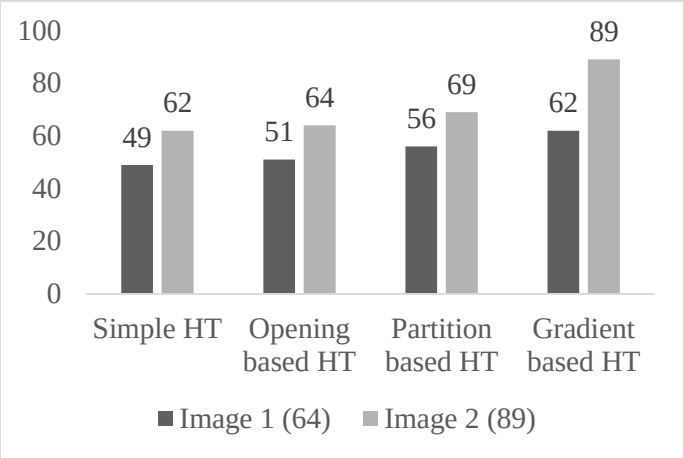

Figure 12. Number of detected fibers (out of 64 and 89 fibers in image 1 and image 2 respectively)

From figure 12, we can see that the performance of the simple HT and the opening method is very close, whereas the partitioning HT is slightly better. The gradient base HT has the highest accuracy. Indeed, this method can accurately detect almost all the fibers from images.

CONCLUSION AND DISCUSSION

In this paper, we deal with the problem of extracting fibers from the SEM images of fiber reinforced composites. We proposed four different methods based on various image processing techniques, the opening method, the simple HT method, the partitioning based HT method, and the gradient based HT method. To demonstrate and compare the effectiveness of these methods, a simulation based case study has been performed using simulated SEM images with different fiber densities. The results show that the simple HT method has the worst performance. The partitioning step can improve the detection accuracy. However, its effectiveness is monotonically decreasing as the fiber density increases. The gradient based HT method has the highest detection accuracy in all four fiber density levels. The opening method is very stale and will not be affected much by the fiber density. A real case study was also conducted to illustrate the applicability of these methods.

There are some open issues for future investigation in the fiber extraction from SEM images. First of all, the proposed methods are only applicable when the fibers are straight. However, in many fiber reinforced composites, the fibers are long in length and curved in shape. Second, due to resolution or contrast issue, the fibers may be difficult to recognize from the background of the SEM image. How to accurately extract fibers in such circumstance needs to be investigated.

REFERENCES

[1] K. L. Pickering, M. A. Efendy, and T. M. Le, "A review of recent developments in natural fibre composites and their mechanical performance," *Composites Part A: Applied Science and Manufacturing*, vol. 83, pp. 98-112, 2016.

[2] C. E. Bakis, L. C. Bank, V. Brown, E. Cosenza, J. Davalos, J. Lesko, A. Machida, S. Rizkalla, and T. Triantafillou, "Fiber-reinforced polymer composites for construction—State-of-the-art review," *Journal of composites for construction*, vol. 6, pp. 73-87, 2002.

[3] Y. Cao, P. C. Irwin, and K. Younsi, "The future of nanodielectrics in the electrical power industry," *IEEE Transactions on Dielectrics and Electrical Insulation*, vol. 11, pp. 797-807, 2004.

[4] D. M. Frangopol and S. Recek, "Reliability of fiber-reinforced composite laminate plates," *Probabilistic Engineering Mechanics*, vol. 18, pp. 119-137, 2003.

[5] V. Tomer and C. Randall, "High field dielectric properties of anisotropic polymer-ceramic composites," *Journal of Applied Physics*, vol. 104, p. 074106, 2008.

[6] C. Bowen, R. Newnham, and C. Randall, "Dielectric properties of dielectrophoretically assembled particulate-polymer composites," *Journal of materials research*, vol. 13, pp. 205-210, 1998.

[7] H. Tang, Y. Lin, and H. A. Sodano, "Enhanced energy storage in nanocomposite capacitors through aligned PZT nanowires by uniaxial strain assembly," *Advanced Energy Materials*, vol. 2, pp. 469-476, 2012.

[8] J. Wu, S. Zhou, and X. Li, "Acoustic emission monitoring for ultrasonic cavitation based dispersion process," *Journal of Manufacturing Science and Engineering*, vol. 135, p. 031015, 2013.

[9] J. Wu, S. Zhou, and X. Li, "Ultrasonic Attenuation Based Inspection Method for Scale-up Production of A206–Al2O3 Metal Matrix Nanocomposites," *Journal of Manufacturing Science and Engineering*, vol. 137, p. 011013, 2015.

[10] Y. Liu, J. Wu, S. Zhou, and X. Li, "Microstructure modeling and ultrasonic wave propagation simulation of A206–Al2O3 metal matrix nanocomposites for quality inspection," *Journal of Manufacturing Science and Engineering*, vol. 138, p. 031008, 2016.

[11] J. Wu, Y. Liu, and S. Zhou, "Bayesian Hierarchical Linear Modeling of Profile Data With Applications to Quality Control of Nanomanufacturing," *IEEE Transactions on Automation Science and Engineering*, vol. 13, pp. 1355-1366, 2016.

[12] B. A. Bednarcyk, J. Aboudi, and S. M. Arnold, "Analysis of fiber clustering in composite materials using high-fidelity multiscale micromechanics," *International Journal of Solids and Structures*, vol. 69, pp. 311-327, 2015.

[13] C. Park, J. Z. Huang, D. Huitink, S. Kundu, B. K. Mallick, H. Liang, and Y. Ding, "A multistage, semi-automated procedure for analyzing the morphology of

nanoparticles," *IIE Transactions,* vol. 44, pp. 507-522, 2012.
[14] C. Park, J. Z. Huang, J. X. Ji, and Y. Ding, "Segmentation, inference and classification of partially overlapping nanoparticles," *IEEE transactions on pattern analysis and machine intelligence,* vol. 35, pp. 1-1, 2013.
[15] K. M. Kam, L. Zeng, Q. Zhou, R. Tran, and J. Yang, "On assessing spatial uniformity of particle distributions in quality control of manufacturing processes," *Journal of Manufacturing Systems,* vol. 32, pp. 154-166, 2013.
[16] L. Zeng, Q. Zhou, M. P. De Cicco, X. Li, and S. Zhou, "Quantifying boundary effect of nanoparticles in metal matrix nanocomposite fabrication processes," *IIE Transactions,* vol. 44, pp. 551-567, 2012.
[17] K. Kimura, S. Kikuchi, and S.-i. Yamasaki, "Accurate root length measurement by image analysis," *Plant and Soil,* vol. 216, pp. 117-127, 1999.
[18] K. Kawabata, Y. Komori, T. Mishima, and H. Asama, "An asbestos fiber detection technique utilizing image processing based on dispersion color," *Particulate Science and Technology,* vol. 27, pp. 177-192, 2009.
[19] T. Peng, A. Balijepalli, S. K. Gupta, and T. W. LeBrun, "Algorithms for extraction of nanowire lengths and positions from optical section microscopy image sequence," *Journal of Computing and Information Science in Engineering,* vol. 9, p. 041007, 2009.
[20] Y. J. Jeon, H. W. Kang, S. H. Ko, and H. J. Sung, "Pattern analysis of aligned nanowires in a microchannel," *Measurement Science and Technology,* vol. 24, p. 035303, 2013.
[21] J. Illingworth and J. Kittler, "A survey of the Hough transform," *Computer vision, graphics, and image processing,* vol. 44, pp. 87-116, 1988.
[22] R. M. Haralick, S. R. Sternberg, and X. Zhuang, "Image analysis using mathematical morphology," *IEEE transactions on pattern analysis and machine intelligence,* pp. 532-550, 1987.
[23] P. V. Hough, "Method and means for recognizing complex patterns," 1962.
[24] R. O. Duda and P. E. Hart, "Use of the Hough transformation to detect lines and curves in pictures," *Communications of the ACM,* vol. 15, pp. 11-15, 1972.
[25] T. Zhang and C. Y. Suen, "A fast parallel algorithm for thinning digital patterns," *Communications of the ACM,* vol. 27, pp. 236-239, 1984.
[26] H. Freeman, "Computer processing of line-drawing images," *ACM Computing Surveys (CSUR),* vol. 6, pp. 57-97, 1974.
[27] H. Freeman and R. Shapira, "Determining the minimum-area encasing rectangle for an arbitrary closed curve," *Communications of the ACM,* vol. 18, pp. 409-413, 1975.
[28] E. Bribiesca and A. Guzman, "How to describe pure form and how to measure differences in shapes using shape numbers," *Pattern Recognition,* vol. 12, pp. 101-112, 1980.
[29] E. Bribiesca, "Arithmetic operations among shapes using shape numbers," *Pattern Recognition,* vol. 13, pp. 123-137, 1981.
[30] P. R. Reddy, V. Amarnadh, and M. Bhaskar, "Evaluation of stopping criterion in contour tracing algorithms," *International Journal of Computer Science and Information Technologies,* vol. 3, pp. 3888-3894, 2012.